Force detection in optical tweezers using backscattered light

J. H. G. Huisstede, K. O. van der Werf, M. L. Bennink, V. Subramaniam

Biophysical Engineering and MESA+ institute for nanotechnology, Department of Science and Technology, University of Twente, P.O. Box 217, 7500 AE Enschede, The Netherlands

v.subramaniam@utwente.nl

Abstract: In force-measuring optical tweezers applications the position of a trapped bead in the direction perpendicular to the laser beam is usually accurately determined by measuring the deflection of the light transmitted through the bead. In this paper we demonstrate that this position and thus the force exerted on the bead can be determined using the backscattered light. Measuring the deflection for a $2.50\mu m$ polystyrene bead with both a position sensitive detector (PSD) and a quadrant detector (QD) we found that the linear detection range for the PSD is approximately twice that for the QD. In a transmission-based setup no difference was found between both detector types. Using a PSD in both setups the linear detection range for $2.50\mu m$ beads was found to be approximately $0.50\mu m$ in both cases. Finally, for the reflection-based setup, parameters such as deflection sensitivity and linear detection range were considered as a function of bead diameter (in the range of $0.5-2.5\mu m$). $140pN$ was the largest force obtained using $2.50\mu m$ beads.

OCIS codes: (120.4640) Optical instruments, (290.1350) Backscattering, (170.4520) Optical confinement and manipulation

References and links

1. A. Ashkin, "Acceleration and trapping of particles by radiation pressure," Phys. Rev. Lett. **24,** 156–159 (1970).
2. A. Ashkin, "Optical trapping and manipulation of neutral particles using lasers," Natl. Acad. Sci. USA **94,** 4853–4860 (1997).
3. A. Ashkin and J.M. Dziedzic, "Optical trapping and manipulation of viruses and bacteria," Science **235,** 1517–1520 (1987).
4. M.S.Z. Kellermayer, S.B. Smith, H.L. Granzier and C. Bustamante, "Folding-unfolding transitions in single titin molecules characterized with laser tweezers," Science **276,** 1112–1116 (1997).
5. M.L. Bennink, S.H. Leuba, G.H. Leno, J. Zlatanova, B.G. de Grooth and J.Greve, "Unfolding individual nucleosomes by stretching single chromatin fibers with optical tweezers," Nat. Struct. Biol. **8,** 606–610 (2001).
6. C. Bustamante and Y. Cui, "Pulling a single chromatin fiber reveals the forces that maintain its higher-order structure," Proc. Natl. Acad. Sci. **97,** 127–132 (2000).
7. S.M. Block, L.S.B. Goldstein and B.J. Schnapp, "Bead movement by single kinesin molecules studied with optical tweezers," Nature (London) **348,** 348–352 (1990).
8. A.D. Mehta, M. Rief, J.A. Spudich, D.A. Smith and R.M. Simmons, "Single-molecule biomechanics with optical methods," Science **283,** 1689–1695 (1999).
9. L.P. Ghislain, N.A. Switz and W.W. Webb, "Measurement of small forces using an optical trap," Rev. Scient. Instr. **65,** 2762–2768 (1994).
10. R.M. Simmons, J.T. Finer, S. Chu and J.A. Spudich, "Quantitative measurements of force and displacement using an optical trap," Biophys. J. **70,** 1813–1822 (1996).
11. A. Pralle, M. Prummer, E.-L. Florin, E.H.K. Stelzer and J.K.H. Hörber, "Three-Dimensional high-resolution particle tracking for optical tweezers by forward scattered light," Micr. Res. Techn. **44,** 378–386 (1999).

#6016 - $15.00 US Received 14 December 2004; revised 8 February 2005; accepted 8 February 2005

12. A. Rohrbach and E.H.K. Stelzer,"Three-dimensional position detection of optically trapped dielectric particles," J. Appl. Phys. **91** 5474–5488 (2002).
13. J.K. Dreyer, K. Berg-Sørensen and L. Oddershede,"Improved axial position detection in optical tweezers measurements," Appl. Opt. **43,** 1991–1995 (2004).
14. I.M. Peters, Y. van Kooyk, S.J. van Vliet, B.G. de Grooth, C.G. Figdor and J. Greve, "3D single-particle tracking and optical trap measurements on adhesion proteins," Cytometry **36,** 189–194 (1999).
15. M.E.J. Friese, H. Rubinsztein-Dunlop, N.R. Heckenberg and E.W. Dearden, "Determination of the force constant of a single-beam gradient trap by measurement of backscattered light," Appl. Opt. **35,** 7112–7116 (1996).
16. J. Dapprich and N. Nicklaus, "DNA attachment to optically trapped beads in microstructures monitored by bead displacement," Bioimaging **6,** 25–32 (1998).
17. F. Gittes and C.F. Schmidt, "Thermal noise limitations on micromechanical experiments," Eur. Biophys. J. **27,** 75–81 (1998).
18. T. Wohland, A. Rosin and E.H.K. Stelzer, "Theoretical determination of the influence of the polarization on forces exerted by optical tweezers," Optik **102,** 181–190 (1996).
19. F. Reif, *Fundamentals of statistical and thermal physics* (McGraw-Hill, New York, 1965).
20. K. Svoboda and S.M. Block, "Biological applications of optical forces," Annu. Rev. Biophys. Biomol. Struct. **23,** 247–285 (1994).
21. K. Visscher and S.M. Block, "Versatile optical traps with feedback control," Meth. in Enzym. **298,** 460–489 (1998).
22. A. Ashkin, "Forces of a single-beam gradient laser trap on a dielectric sphere in the ray optics regime," Bioph. J. **61,** 569–582 (1992).
23. S.B. Smith, Y. Cui and C. Bustamante, "Overstretching B-DNA: the elastic response of individual double-stranded DNA molecules," Science **271,** 795–799 (1996).

1. Introduction

Optical tweezers (OT) have become a widely used tool in biophysics since their introduction by Ashkin approximately 20 years ago [1, 2]. The technique employs a high intensity laser beam that is focused down to a diffraction-limited spot. Due to the interaction of light with matter, (sub)micron particles can be trapped at a position close to the focus. This makes the OT an excellent tool for capturing and moving particles around [3]. In addition to the ability to hold particles at a certain position, the optical tweezers can be used to measure forces exerted on the trapped bead. When spherically shaped beads are used, the force exerted on the bead is linearly related to the displacement of the bead from the trap center. Forces of up to $100\,pN$ were achieved using micron-sized latex or polystyrene beads which makes the technique excellent for measuring forces involved in stretching individual molecules such as titin [4], DNA and proteins or complexes thereof, [5, 6] and forces involved in the action of molecular motors [7, 8].

The lateral position of the trapped bead, i.e. the position in the direction perpendicular to the laser beam, with respect to the trap center, and thus the force acting on the bead in this direction, can be accurately measured using the deflection of the transmitted laser light [9, 10]. In addition it is shown in literature that the axial position of the trapped bead is related to the forward scattered light intensity, enabling three dimensional bead tracking [11, 12, 13]. For most single molecule stretching experiments, measuring the force in one dimension is sufficient, whereas for experiments involving for instance elasticity measurements of a cell membrane [14], three dimensional force measuring is acquired. Our future application involves stretching single dsDNA molecules and therefore we consider only forces in the lateral direction in this article. Instead of measuring the refraction of the forward scattered light, we report a setup in which the backscattered laser trapping light was used for lateral force detection. In Fig. 1 both detection principles are schematically shown. In the reflection-based setup a condenser lens is no longer required and this makes the setup more versatile. For example, experiments using a bead coupled to a cell membrane to measure local elastic properties of the membrane will benefit from using the reflected trapping light, because the deflection of the transmitted light is affected by the cellular environment [14]. This mode also enables the addition of other types of

#6016 - $15.00 US Received 14 December 2004; revised 8 February 2005; accepted 8 February 2005

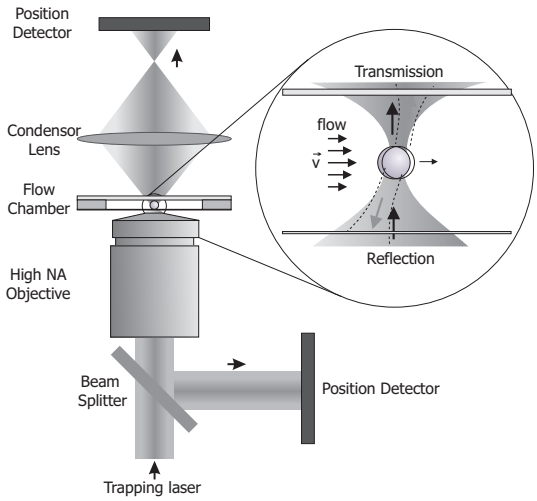

Fig. 1. Schematic overview of the optical trap in which the detection in transmission and reflection is indicated. For the transmission detection a condenser lens collects a part of the light transmitted by a trapped bead and directs it onto a position detector, which is positioned slightly behind the conjugate back focal plane of the condenser lens. In reflection the backscattered light is directed on a position detector using a beam splitter.

probes such as an AFM tip or a NSOM tip to the OT, to combine these techniques.

In the literature the use of the backscattered light as a signal for force detection is mentioned, but is not discussed extensively [15, 16]. Here we describe the details of the reflection-based setup, where we consider the system properties only for lateral displacements of a trapped bead. Hydrodynamic forces are used as a method to initiate a bead displacement to measure the deflection of the backscattered light as a function of bead position. We briefly describe the power spectrum method [17], often applied in OT, to calibrate the trap stiffness. This calibration is required in order to convert the position of the trapped bead, measured as a deflection signal, to the force exerted on this bead.

In Section 3 we compare the use of a position sensitive detector and a quadrant detector to measure the deflection of the backscattered light as a function of the position of a $2.50\mu m$ trapped bead, where we focus on the linear detection regime of both detectors. The same study has been performed on a transmission-based setup available in our laboratory. Although both position detectors are widely used in OT, to our knowledge there is no systematic comparison of the two detectors in the literature. Furthermore this investigation allows comparison of the reflection-based setup with its transmission-based counterpart. We also acquired and compared power spectra in both setups for the case where a bead was trapped and for no bead, indicating the noise limitations.

Finally we show deflection curves for polystyrene beads of four different bead sizes in the range of $0.5-2.5\mu m$ measured with the reflection-based setup. By determining the trap stiffness for each bead size the linear position detection range can be expressed as a force range. We also determined the deflection sensitivities for the different bead sizes. From these results an appropriate bead size for future applications can be chosen.

#6016 - $15.00 US Received 14 December 2004; revised 8 February 2005; accepted 8 February 2005

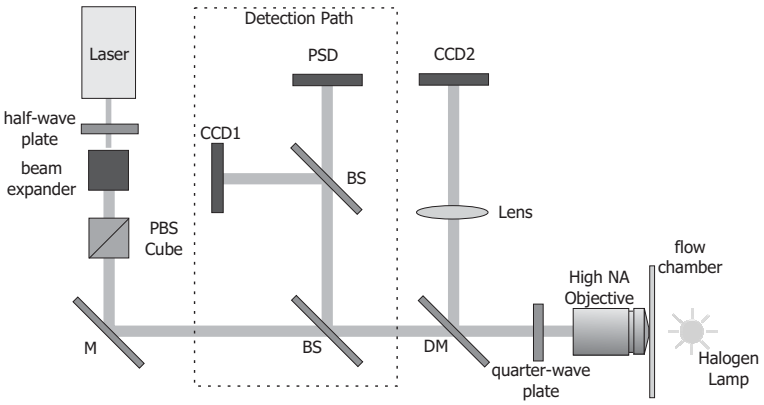

Fig. 2. Schematic representation of the reflection-based optical tweezers setup. A beam expander provides overfilling of the back-aperture of a high NA objective. The laser power at this aperture is controlled by combining a half-wave plate and a polarizing beam splitter cube. A quarter-wave plate just in front of the objective provides circularly polarized light for the trap. A beam splitter directs the backscattered light onto a position sensitive detector where a second beam splitter in the detection path (indicated with the dotted line) enables visualizing the reflection pattern on a CCD camera (CCD1). A halogen lamp provides white light illumination for imaging the trapped bead via a dichroic mirror (DM) on a second CCD camera (CCD2).

2. Materials and methods

2.1. Experimental apparatus

A diode-pumped Nd:YAG (CrystaLaser IRCL-2W-1064) laser with an output power of 2W at λ = 1064 nm (TEM_{00}) serves as the trapping laser. A beam expander is used to overfill the objective entrance in order to optimize the optical tweezers efficiency [9]. A combination of a half-wave plate and a polarizing beam splitter cube is used to control the laser power at this entrance as shown in Fig. 2. A 100x, infinity-corrected, water-immersion objective (Leica N PLAN) with a NA of 1.20 yields a steep gradient in the electric field to trap small dielectric particles. This objective simultaneously collects the backscattered light from the trapped particle, directing the light on to a position sensitive detector (UDT-DLS10) or a quadrant detector (Hamamatsu, S5891) using a beam splitter (90/10). A second beam splitter (90/10) in the detection path is used to visualize the backscattered light with a charge coupled device camera (Panasonic F15) with an active area of 8.5*x*6.4 mm^2 (CCD1 in Fig. 2). A quarter-wave plate placed in front of the objective converts the incident p-polarized laser light into circularly polarized light, providing an equal trap stiffness in both lateral directions [18]. The maximum trapping laser power at the back aperture of the objective is 550 mW. In this case the power of the collected backscattered light at the position sensitive detector is in the range of 100-500 μW, dependent on bead size. A halogen lamp is used as light source for the white light detection. Using a dichroic mirror an image is formed on a second charge coupled device camera (CCD2 in Fig. 2) with an active area of 6.4*x*4.8 mm^2. For the experiments polystyrene beads are used with diameters of 0.45μm (Polysciences, carboxylated), 1.07μm (Polysciences, carboxylated), 1.44μm (Polysciences) and 2.50μm (Bangs Laboratory, carboxylated).

#6016 - $15.00 US Received 14 December 2004; revised 8 February 2005; accepted 8 February 2005

2.2. Force calibration

Conceptually the motion of a trapped bead can be described as if it is connected by a Hookean spring to the center of the trap. The force, F_{ext}, acting on the bead is proportional to the position of the bead, Δx, relative to its center position, according to $F_{ext} = k_{tr}\Delta x$, where k_{tr} denotes the trap stiffness.

The position of the bead is detected by using a position detector measuring the deflection of the backscattered laser light. We used hydrodynamic forces to create a bead displacement, which allowed the deflection to be determined as a function of bead position. A stepwise increase in the flow rate, $\overrightarrow{v}$, within the flow cell, Fig. 1, yields an increase in the drag force acting on a trapped bead with radius r according to

$$\overrightarrow{F}_{drag} = \gamma\overrightarrow{v} = 6\pi\eta r\overrightarrow{v} \tag{1}$$

where η is the dynamic viscosity of the medium (water) surrounding the bead and γ the hydrodynamic drag coefficient described by Stokes' law [19]. All the experiments described in this study are done around $50\mu m$ away from any surface where corrections to Stokes' law can be neglected [17]. By recording white light images of the trapped bead and the position detector signals at different flow rates simultaneously, we can relate the detector output to the position of the bead, which is determined by applying a centroid method to the white light images. The images recorded by the CCD device were calibrated by imaging a line pattern with lines spaced 10 μm from one another. To determine the force acting on the bead, both the bead position and the trap stiffness needs to be determined. For a transmission-based detection system several trap stiffness calibration techniques such as the escape force method, the momentum transfer method, the equipartition method, the drag force method and the power spectrum method have been developed [20, 21]. Here we use the last one.

For beads optically trapped in solution, the fluctuations due to thermal collisions of surrounding molecules can be modelled by the response of the bead to a microscopic random thermal (white-noise) force, expressed by the Langevin equation [17]. The system is strongly overdamped such that the influence of the mass can be neglected in the region of interest ($f < 100kHz$). For such a Brownian harmonic oscillator, where motion takes place at small Reynolds number, the power spectral density of the bead position is given by the Lorentzian expression [17],

$$S_x(f) = \frac{k_bT}{\gamma\pi^2(f_c^2 + f^2)} \tag{2}$$

where k_b is Boltzmann's constant, T the absolute temperature and f the frequency. The trap stiffness, k_{tr}, is related to the cut-off frequency f_c according to $k_{tr} = 2\pi\gamma f_c$. The units of $S_x(f)$ are nm^2/Hz. At low frequencies the power spectral density is approximately constant, given by

$$f \ll f_c \Rightarrow S_x(0) \approx \frac{k_bT}{\gamma\pi^2 f_c^2} = \frac{4\gamma k_bT}{k_{tr}^2} \tag{3}$$

Note that the thermal white-noise force magnitude is given by $S_F(f) = 4\gamma k_bT$ and $S_x(0)$ thus reflects the confinement of the bead, dependent on the trap stiffness. For frequencies $f \gg f_c$ the power spectrum drops as $1/f^2$, indicating free diffusion. Using this model to fit the recorded power spectral density, the trap stiffness can be deduced from the cut-off frequency. The bandwidth of the detection hardware used was limited to $9.7kHz$ using a second-order low pass filter in order to increase the signal-to-noise ratio [17].

#6016 - $15.00 US Received 14 December 2004; revised 8 February 2005; accepted 8 February 2005

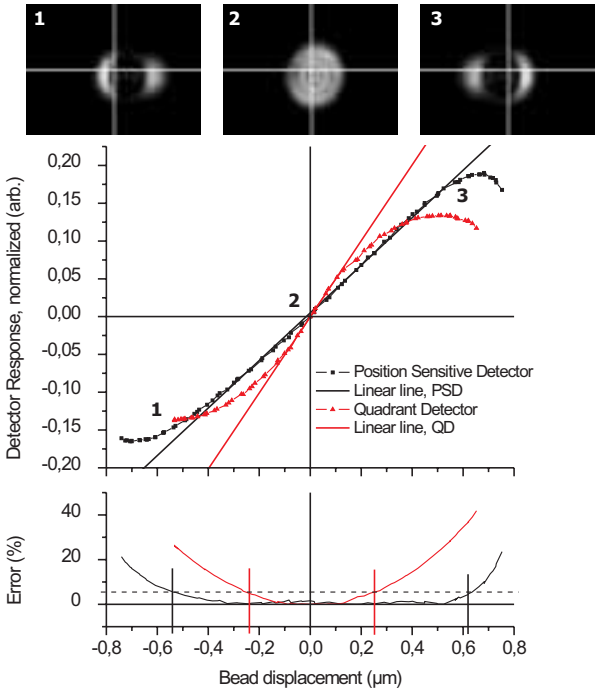

Fig. 3. Comparison between a PSD (black curve) and a QD (red curve) for a reflection-based OT setup. The bead size was $2.50\mu m$. Three images of the reflection pattern are shown, recorded at a bead position of -0.6, 0.0 and $+0.6\mu m$. These positions are also indicated in the deflection curves with the numbers 1, 2 and 3, respectively. The lower error graph indicates the difference between the experimental data and a linear line (also shown), having a slope similar to the slope of the deflection curve around the center position of the bead. The error was calculated as the difference between these two lines, divided by the value of the linear line at $1.0\mu m$, and expressed as a percentage. The dotted line in the error graph indicates an error of 5% used to determine the linear detection range of both the PSD and the QD. As a result the linear range, expressed relatively to the center position of the trapped bead, for the PSD is $0.57\mu m$ and for the QD $0.25\mu m$.

3. Experimental results

3.1. Reflection-based setup: PSD versus QD

For measuring the deflection of a light beam two detector types are commonly used in optical tweezers applications. The first type is a quadrant detector (QD) that measures difference signals from the quadrant segments. The second one is a position sensitive detector (PSD) which determines the center of intensity of the spot on the detector. For $2.50\mu m$ beads the deflection as a function of bead position was acquired using both detectors. The active area of both detectors is $10x10\ mm^2$. The laser power was adjusted such that we were able to exert drag forces high enough to displace the bead over a range of $\sim 0.6\mu m$ relative to its center position within the trap. It was checked that the deflection curve, normalized for the sum signal of the detector, was independent on laser power. Furthermore images were recorded with the CCD camera in the detection path (CCD1 in Fig. 2) visualizing the reflection pattern, and are plotted in Fig. 3. The reflection images shown, were recorded at bead positions $-0.6\mu m$, $0.0\mu m$ and $+0.6\mu m$, indicated in the deflection curve with the numbers 1, 2 and 3 respectively. The slope of the

#6016 - $15.00 US Received 14 December 2004; revised 8 February 2005; accepted 8 February 2005

curve around the center position of the bead was determined. For the PSD this slope is 0.31 and for the QD 0.50 with arbitrary units. In a next step the difference between the experimental data and a linear line having this slope was calculated. Subsequently the difference was divided by the value of the linear line at $1.0\mu m$ and expressed as a percentage, shown in Fig. 3. The linear range was defined as the region in which this deviation is less than 5%. As a result the linear detection range for a $2.50\mu m$ bead measured with a QD is $0.25\mu m$ whereas the range measured with a PSD is $0.57\mu m$. The linear range is expressed relatively to the center position of the trapped bead.

The backscattered reflection pattern of a trapped bead (see Fig. 3) not only shifts when a displacement of the bead is induced, but also changes shape, especially for larger displacements. In the reflection image for a displacement of $0.6\mu m$ the pattern exhibits two high intensity regions. The QD, which measures the intensity difference across a border, shown in the reflection images in Fig. 3 as a white cross, will not measure a movement of the spot at higher bead displacements, because there is no energy transferred across this border due to the black region. Only a relative change in intensity of the two distinct high intensity regions will be detected. The position sensitive detector, on the other hand, determines the center of intensity of the incident spot and circumvents this problem. Another property of the quadrant detector is that the deflection sensitivity is dependent on spot size. The smaller the spot, the higher the deflection sensitivity, expressed in $V/\mu m$. Because the PSD determines the center of energy we found that it is not sensitive for spot size, as expected.

3.2. Transmission-based setup: PSD versus QD

The reflection-based setup was compared with a transmission-based setup available in our laboratory [5]. The laser, the objective and the beam expansion to achieve a slight overfilling of the back aperture of the high NA objective are the same in both setups. Similar to the reflection-based setup a quarter-wave plate was incorporated just in front of the objective. The maximum trapping laser power at the back aperture of the objective was $470mW$. The trapping part of the setup is the same as the reflection-based setup as shown in Fig. 2, with the exception of the detection part. The detection setup for the transmission-based geometry is schematically shown in Fig. 1 where a condenser lens with a NA of 0.90 collects a part of the transmitted light. The position detector is placed slightly behind the conjugate back focal plane of the condenser lens. A polarizing beam splitter is placed in between the condenser lens and the position detector to direct 50% of the transmitted light on a CCD camera (Panasonic F15) for visualization of the transmission pattern. A neutral density filter in front of this beam splitter is used to decrease the laser intensity to measurable levels.

For the transmission-based setup the experiment with the $2.50\mu m$ beads, described in the previous section, was repeated. Although both detectors are widely used for transmission-based setups, we are not aware of a comparison between the PSD and the QD for such a setup. For the transmission-based setup the same position detectors were used as for the reflection-based setup. Following the same procedure as described in the previous section, we acquired images of the transmission pattern, deflection curves (normalized for the sum) using the PSD and the QD and an error graph indicating the difference between the experimental data and a linear line with a slope of the deflection curve around the center position of the bead. From the error graph the linear range was determined by accepting a maximum error of 5%. These results are shown in Fig. 4 where the images of the transmission pattern are recorded at bead position $-0.6\mu m$, $0.0\mu m$ and $+0.6\mu m$, indicated in the deflection curve with the numbers 1, 2 and 3 respectively. The deflection curves are somewhat noisier compared to the reflection-based setup, which is caused by small flow instabilities caused by the pressure system controlling the flow speed. For both position detectors the linear range is $0.45\mu m$. Note that outside the linear range the

#6016 - $15.00 US Received 14 December 2004; revised 8 February 2005; accepted 8 February 2005

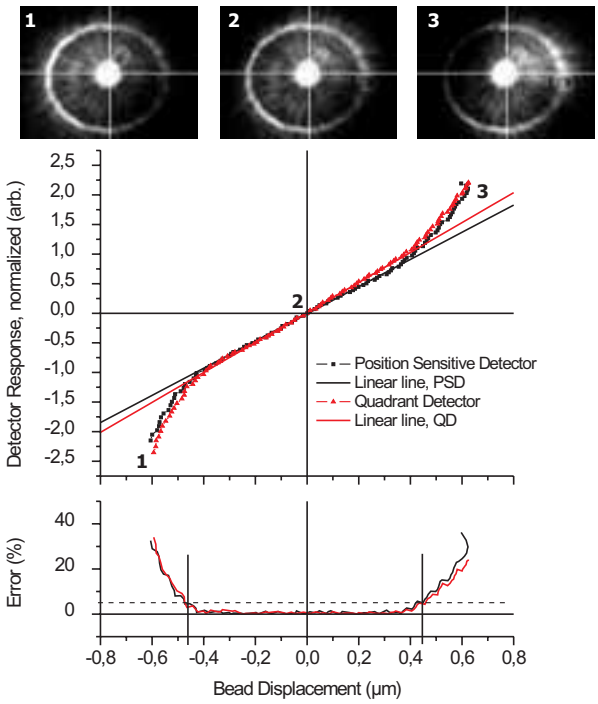

Fig. 4. Comparison between a PSD (black curve) and a QD (red curve) for a transmission-based OT setup. The bead size was $2.50\mu m$. Three images of the reflection pattern are shown, recorded at a bead position of -0.6, 0.0 and $+0.6\mu m$. These positions are also indicated in the deflection curves with the numbers 1, 2 and 3, respectively. The lower error graph indicates the difference between the experimental data and a linear line (also shown), having a slope similar to the slope of the deflection curve around the center position of the bead. The error is calculated in a similar way as done for the reflection-based results shown in Fig. 3. The dotted line in the error graph indicates an error of 5% used to determine the linear detection range of both the PSD and the QD. As a result the linear range for both the PSD and the QD is $0.45\mu m$.

deflection sensitivity increases. Moving the condenser lens to another position does not change this behavior qualitatively.

3.3. Noise limitations both setups

Fig. 5 depicts power spectra for a $2.50\mu m$ bead acquired on both setups using the PSD. In both systems the laser power at the back aperture of the objective was $\sim 170mW$, leading to similar spectra, emphasizing that both setups are comparable. Additional spectra are shown when no bead was trapped. At higher frequencies these spectra are shot-noise limited. The shot-noise level is dependent on the light intensity on the detector. The higher the intensity the higher the signal-to-noise ratio and the lower the shot-noise level. When no bead is trapped there is still a laser signal for the transmission-based setup, but for the reflection-based setup there is none. Therefore the shot-noise level is higher for the reflection-based setup. For the transmission-based setup 1/f-noise and additional peaks are visible in the spectrum at lower frequencies, caused by mechanical and acoustical noise. All the spectra shown are recorded for 21 seconds at a scan rate of $100kHz$. As can be seen from Fig. 5 both setups are limited by the thermal

#6016 - $15.00 US Received 14 December 2004; revised 8 February 2005; accepted 8 February 2005

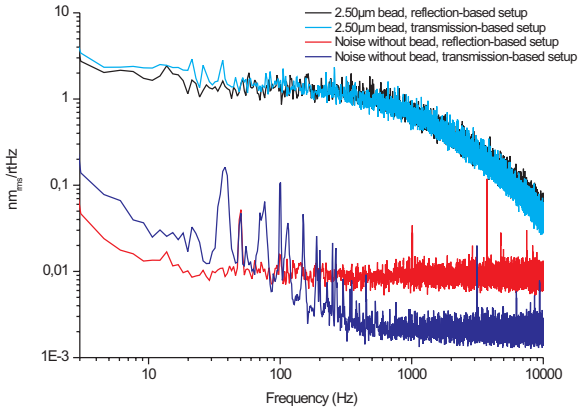

Fig. 5. Spectra for a $2.50\mu m$ bead at $170mW$ laser power acquired in a transmission-based and reflection-based OT setup. Furthermore the noise spectra without a trapped bead is plotted for both setups to pinpoint they are thermal noise limited. When no bead is trapped, for the transmission-based setup there is still a laser signal, but for the reflection-based setup it is not. Therefore the shot-noise limitation visible at higher frequencies, is higher for the reflection-based setup. The transmission-based setup, on the other hand, is still sensitive for mechanical and acoustical noise when no bead is trapped, appearing as 1/f-noise and several peaks for frequencies lower than $1kHz$. The bandwidth of the detection system is 9.7kHz.

noise of the trapped bead.

3.4. Deflection curves for different bead sizes

Having shown that the backscattered laser light can be used to measure the force acting on a trapped bead, we focus on the influence of the bead size on the deflection sensitivity of our detection system and the linear range over which we can detect the position of the bead. The last parameter can be converted into the linear force range with the trap stiffness as conversion factor. Thus by controlling the trap stiffness with the laser power, we are able to control the force range. For future applications of the reflection-based setup it is important to know the linear force range over which we can measure and the dependence of this range on bead size.

Using the drag force method described in Section 2.2 we determined deflection curves for four different bead sizes of 0.45, 1.07, 1.44 and $2.50\mu m$, shown in Fig. 6. For each bead size we recorded deflection curves of multiple beads and the corresponding power spectra of the time signals with a sampling rate of $100kHz$ for a period of 21 seconds. From these results we determined the deflection sensitivity, the linear range and the trap stiffness. These are averaged over a number of beads with the same size and the results are shown in table 1. Both the values for the laser power at the position sensitive detector and the trap stiffness are given for the maximum achievable laser power in our setup, which is $550mW$.

For the $1.07\mu m$ beads the highest trap stiffness was found, which is in agreement with previous results shown by Simmons et al. [10], also for a laser wavelength of $\lambda = 1064nm$. According to Ashkin [22], for Rayleigh particles ($r \ll \lambda$) trapping force depends on r^3. On the other hand, for large particles ($r \gg \lambda$), where the ray optic regime holds, the trap stiffness is decreasing for increasing bead diameter. Our results, which are for sizes of particles in between these regimes, are consistent with these predictions. For the 1.44 and $2.50\mu m$ beads we found the highest deflection sensitivities, $\sim 0.28\mu m$, whereas for the 1.07 and $0.45\mu m$ beads this is

#6016 - $15.00 US Received 14 December 2004; revised 8 February 2005; accepted 8 February 2005

Table 1. Experimental Results for different bead sizes

Bead size (μm)	**Power** (μW)	**Trap stiffness** ($pN/\mu m$)	**Deflection sensitivity** ($V/\mu m$)	**Linear range** (μm)	**Force range** (pN)	**Limitation**
0.45	76 ± 2	334 ± 48	-0.16 $\pm$ 0.02	0.10	33	Escape Force
1.07	418 ± 22	511 ± 31	0.17 $\pm$ 0.01	0.15	77	Escape Force
1.44	464 ± 37	310 ± 18	0.32 $\pm$ 0.03	0.24	74	Reflection pattern
2.50	235 ± 59	242 ± 7	0.28 $\pm$ 0.02	0.57	138	Reflection pattern

a factor 2 lower. Note that these values are normalized for their sum value and therefore independent on laser power as discussed in Section 3.1. A remarkable result is the change in sign of the deflection sensitivity for the $0.45\mu m$, compared with the deflection sensitivities for the other beads.

The linear range for the $2.50\mu m$ and the $1.44\mu m$ beads are determined in the same way as discussed in Section 3.1. For these beads the linear range is limited by the shape of the reflection pattern at large displacements, whereas for the $1.07\mu m$ and $0.45\mu m$ beads the maximum displacement is limited by the escape force, which is the maximum force that can be applied on the bead just before it is pushed out of the trap. The largest linear range is found for the $2.50\mu m$ beads, which is $0.57\mu m$. For the $1.44\mu m$ beads the linear range was $0.24\mu m$. For the 1.07 and $0.45\mu m$ beads the linear range is found to be $0.15\mu m$ and $0.10\mu m$ respectively.

As a last step the linear range is converted to force range via the trap stiffness. For the $2.50\mu m$ bead this force range with a value of $138pN$ is the largest, for both the $1.44\mu m$ and $1.07\mu m$ beads the maximum force that can be measured is $\sim 75pN$. Although the linear range for the $1.44\mu m$ bead is higher, the force range is analogous to the range for the $1.07\mu m$ due to its higher trap stiffness. The maximum force that can be measured with $0.45\mu m$ beads was found to be $33pN$. Besides the achievable force range the force resolution of the detection system should be taken into account. If the system is limited by thermal motion of the trapped bead, which is the case in our setup, the force resolution is dependent on the drag coefficient (and therefore on bead size) and the detection bandwidth ($9.7kHz$ in our case), but not on trap stiffness [17]. Having the same detection bandwidth the force resolution will decrease with decreasing bead size.

Applying the reflection-based setup in the future to for instance single molecules studies on dsDNA, where at least a force level of $\sim 70pN$ should be achieved to identify a single molecule [23], the use of $2.50, 1.44$ and $1.07\mu m$ beads are an appropriate choice.

4. Conclusions

The use of a PSD instead of a QD in the reflection-based setup turned out to be beneficial for the linear position detection range of a trapped bead. For $2.50\mu m$ beads the linear range was $0.57\mu m$ using a PSD, while for a QD this range was found to be $0.25\mu m$, more than a factor 2 difference. For a transmission-based setup, with a similar trap configuration as the reflection-based setup, we found that using a PSD and a QD in both cases the linear range was $0.45\mu m$ for $2.50\mu m$ beads. This means that the reflection-based setup using a PSD as position detector is comparable with the transmission-based setup, where we showed that the position detection in both setups is limited by the thermal noise of the trapped bead. For future applications of the reflection-based setup the influence of bead size on linear force range was investigated. It turned out that the highest force range of $138pN$ could be achieved with $2.50\mu m$ beads. Using smaller beads we found that the force range decreases.

#6016 - $15.00 US Received 14 December 2004; revised 8 February 2005; accepted 8 February 2005

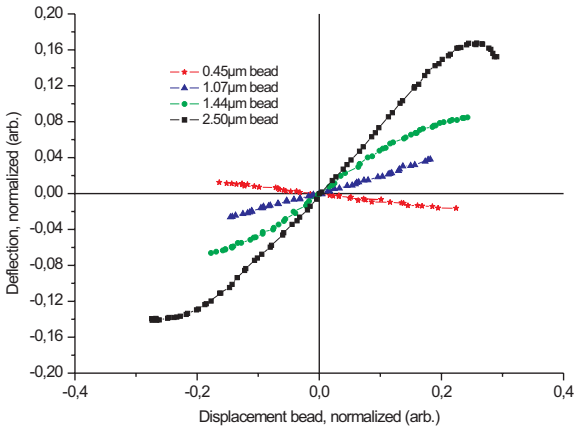

Fig. 6. Position sensitive detector signal as a function of the bead position for different bead sizes, all acquired at $225mW$ laser trap power. For the 1.44 and $2.50\mu m$ bead the linear range is determined by the shape of the reflection pattern. The linear range for the 0.45 and $1.07\mu m$ bead is determined by the escape force, the maximum force that can be applied on the bead before it is pushed out of the trap.

Acknowledgments

This work is supported by the MESA+ institute.

#6016 - $15.00 US Received 14 December 2004; revised 8 February 2005; accepted 8 February 2005